**SUPPLEMENTAL MATERIAL**

# A common variant alters SCN5A:miR-24 interaction and associates with heart failure mortality

Xiaoming Zhang, Jin-Young Yoon, Michael Morley, Jared M. McLendon, Kranti A. Mapuskar, Rebecca Gutmann, Haider Mehdi, Heather L. Bloom, Samuel C. Dudley, Patrick T. Ellinor, Alaa A. Shalaby, Raul. Weiss, W.H. Wilson Tang, Christine S. Moravec, Madhurmeet Singh, Ann L. Taylor, Clyde W. Yancy, Arthur M. Feldman, Dennis M. McNamara, Kaikobad Irani, Douglas R. Spitz, Patrick Breheny, Kenneth Margulies, Barry London*, and Ryan L. Boudreau*

Supplemental materials include:

**Supplemental Figure 1**

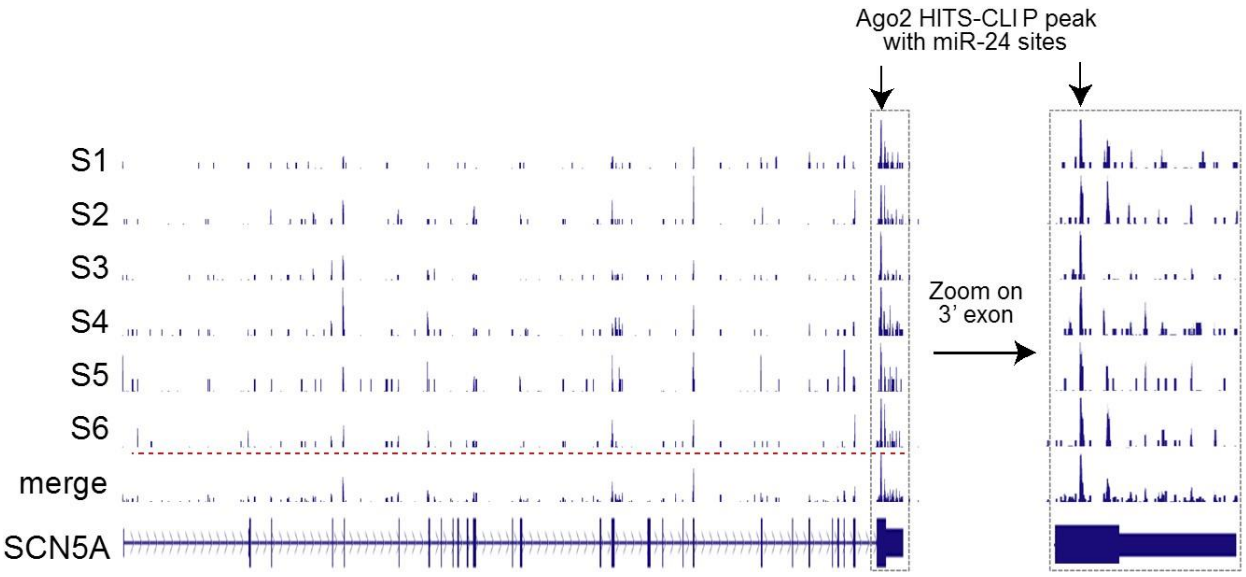


**Supplemental Figure 1. Human cardiac Ago2 binding profile across the *SCN5A* locus.** UCSC Genome Browser screen-capture images of human cardiac Ago2 HITS-CLIP data show the positional read coverage for each sample (S1-S6) and S1-S6 merged across the *SCN5A* locus; the annotated major transcript isoform is diagrammed below. The data illustrate that the Ago2 binding site of interest corresponding to miR-24 is the most robust and reproducible peak within the entire *SCN5A* transcript (red-dotted line in "merge" track). A zoomed image (right) shows the position of this peak within the terminal coding exon; dotted boxed region spans ~3.6kb.

**Supplemental Figure 2**

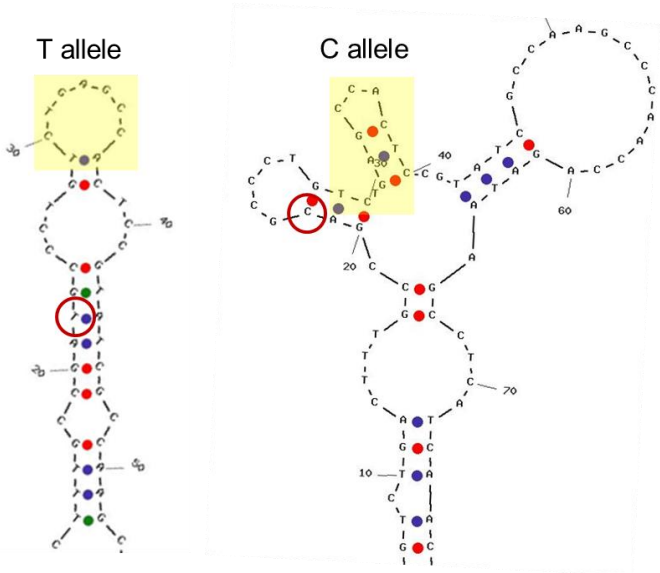


| Allele | dG duplex | dG open | ddG |
|---|---|---|---|
| T | -23.87 | -10.05 | -13.81 |
| C | -23.87 | -7.99 | -15.87 |

**Supplemental Figure 2. Computational modeling of the effect of rs1805126 genotype on *SCN5A* local mRNA structure and targeting by miR-24.** Predictive RNA structure analysis using UNAfold was performed on ~250-nts of *SCN5A* mRNA sequence centered on rs1805126 (red open-circle), revealing a genotype-specific structure that alter the miR-24 binding region (seed highlighted in yellow; refer to **Figure 1A**). The table summarizes PITA microRNA targeting prediction results which indicate that miR-24 binding to the C allele is more energetically favorable (i.e. lower ddG). Note dG and ddG are delta-G and delta-delta-G thermodynamic energies of miR-target binding (duplex), target site accessibility (open), and the difference (ddG).

**Supplemental Figure 3**

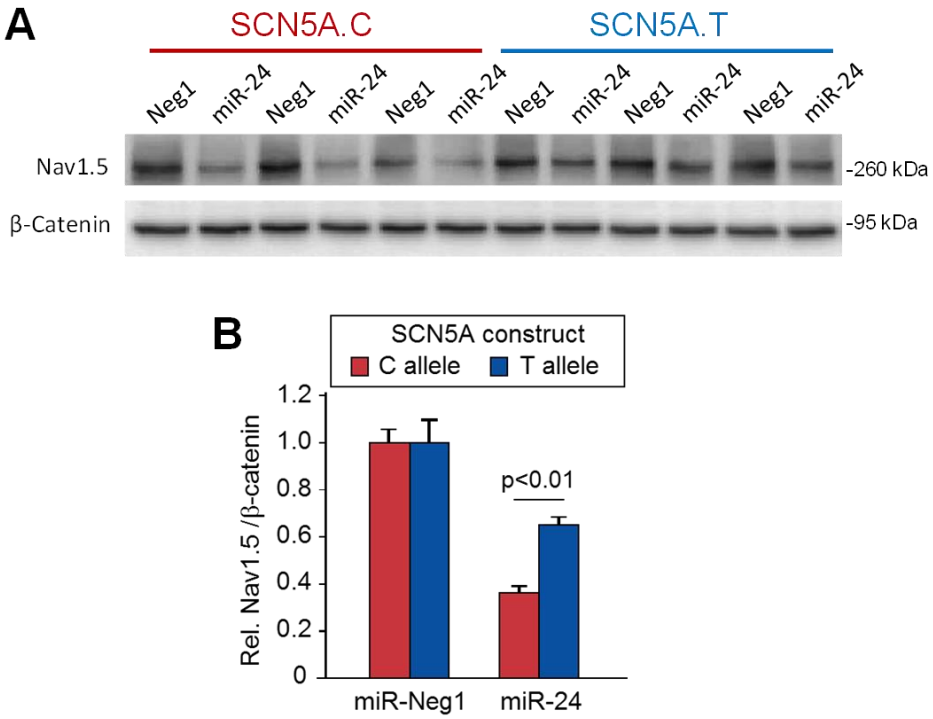


**Supplemental Figure 3. Effect of rs1805126 genotype on miR-24 mediated SCN5A suppression in human HEK293 cells.** The effect of miR-24 on *SCN5A* expression, and the potential impact of rs1805126 on this interaction, was tested in cell culture experiments. Human HEK293 cells were co-transfected in triplicate with synthetic pre-miRs (4 nM) and human full-length *SCN5A* expression plasmids harboring either the C or T allele for rs1805126. At 48 h post-transfection, western blot (**A**) and densitometry analysis (**B**) were performed to measure plasmid-derived $Na_v1.5$ protein expression; as observed in mouse N2a cell studies (**Figure 1B,C**), the C allele was suppressed to a greater degree relative to the T allele. Data are represented as mean +/- SEM (n=3), and p-values were obtained using two-tailed unpaired t-test comparing the indicated groups.

## Supplemental Figure 4

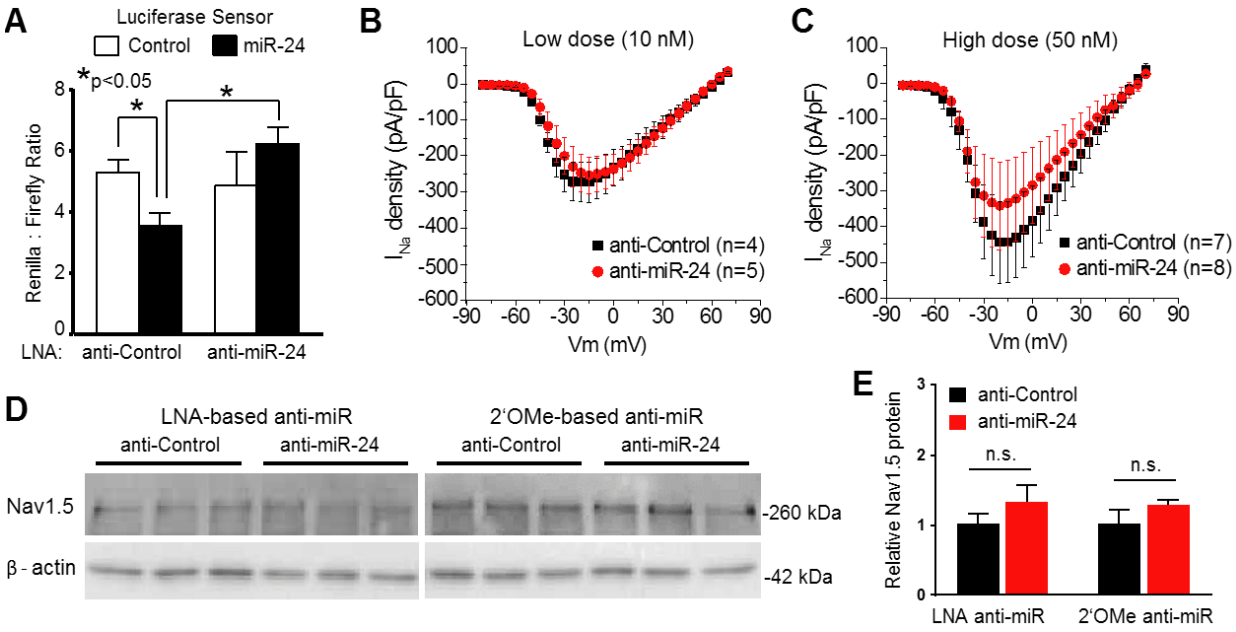


**Supplemental Figure 4. Effects of miR-24 inhibition on *SCN5A* expression and function in neonatal rat cardiomyocytes.** (**A**) NRCMs were co-transfected with LNA-based anti-miR oligonucleotides along with either a control dual luciferase plasmid or a miR-24 dual luciferase sensor plasmid that harbors three miR-24 sites in the Renilla luciferase 3'UTR. (**B,C**) NRCMs were co-transfected with anti-miRs (low and high doses) along with a GFP expression plasmid. $Na^+$ current in GFP-positive cells was measured 2-4 days later using patch-clamp; current-voltage relationship plots for Na+ currents are shown. (**D,E**) NRCMs were transfected with anti-miRs (LNA- or 2'OMe-based, at 50 nM), and 72 hours later, endogenous *SCN5A* protein levels were measured by western blot (**D**) coupled with densitometry analysis (**E**, n=3 total biological replicates per treatment; mean +/- SEM) is plotted. Pre-miR-29 and –Neg1 serve as negative controls, and beta-actin or GAPDH levels were used for normalization. P-values were determined using unpaired two-tailed t-tests; n.s. denotes not significant (i.e. p>0.05).

## Supplemental Figure 5

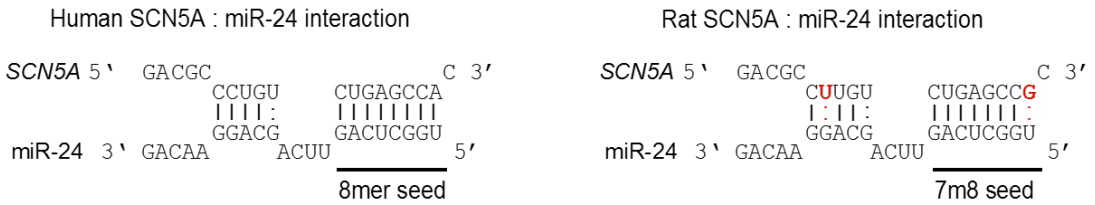


| PITA parameter | Human | Rat | Effect interpretation |
|---|---|---|---|
| dG hybridization energy | -23.9 | -22.5 | Rat mRNA is not bound as strongly by miR-24 |
| dG to open mRNA | -10.0 | -10.5 | miR-24 site in rat SCN5A is not as easily accessed |
| ddG (open and bind) | -13.8 | -12.0 | In sum, rat is a worse substrate for miR-24 binding |

**Supplemental Figure 5. Comparison of predictive miR-24 targeting capacity on human versus rat *SCN5A* mRNAs.** Top, schematics showing miR-24 hybridization to the target site of interest in both human and rat *SCN5A* mRNAs. Red-highlighted nucleotide differences in rat (versus human) *SCN5A* mRNA sequence cause destabilizing G:U wobble base pairing, which downgrades the seed-type to a 7m8 (compared to stronger 8mer in human), and further weakens compensatory binding outside of the seed region. Bottom, table summarizing PITA output data derived from analyzing local human and rat SCN5A mRNA sequences (~400 nucleotides centered on the seed).

**Supplemental Figure 6**

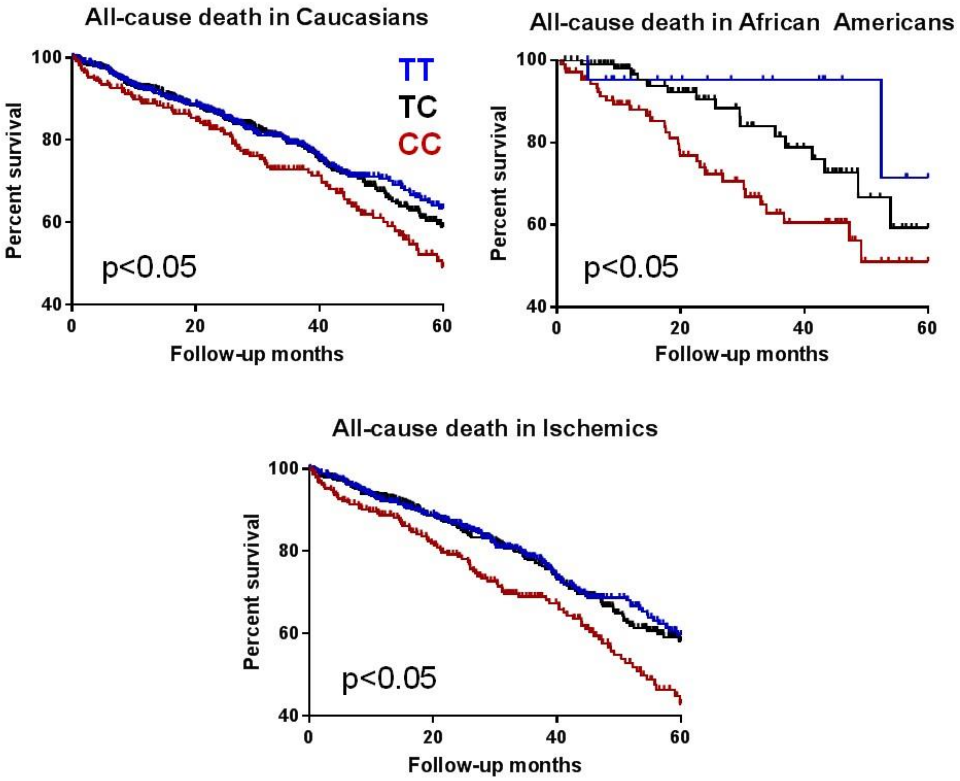


**Supplemental Figure 6. Association of rs1805126 genotype with all-cause death in heart failure patient sub-groups.** Sub-group analyses were performed to assess if whole-cohort analyses might be confounded by other variables that may influence heart failure outcomes (e.g. racial disparities or etiology; subjects with ischemic, versus idiopathic, cardiomyopathy generally have higher mortality risk). Kaplan-Meier curves for overall survival rates from all-cause death show that, in each of the indicated sub-groups, homozygous CC individuals had significantly poorer survival outcomes relative to the other genotypes (i.e. T allele carriers). P-values were obtained using log-rank test. Cohort sizes (TT, TC and CC, respectively) are as follows: Caucasians (495, 502, 230), African Americans (26, 110, 115), and ischemics (381, 447, 235).

**Supplemental Figure 7**

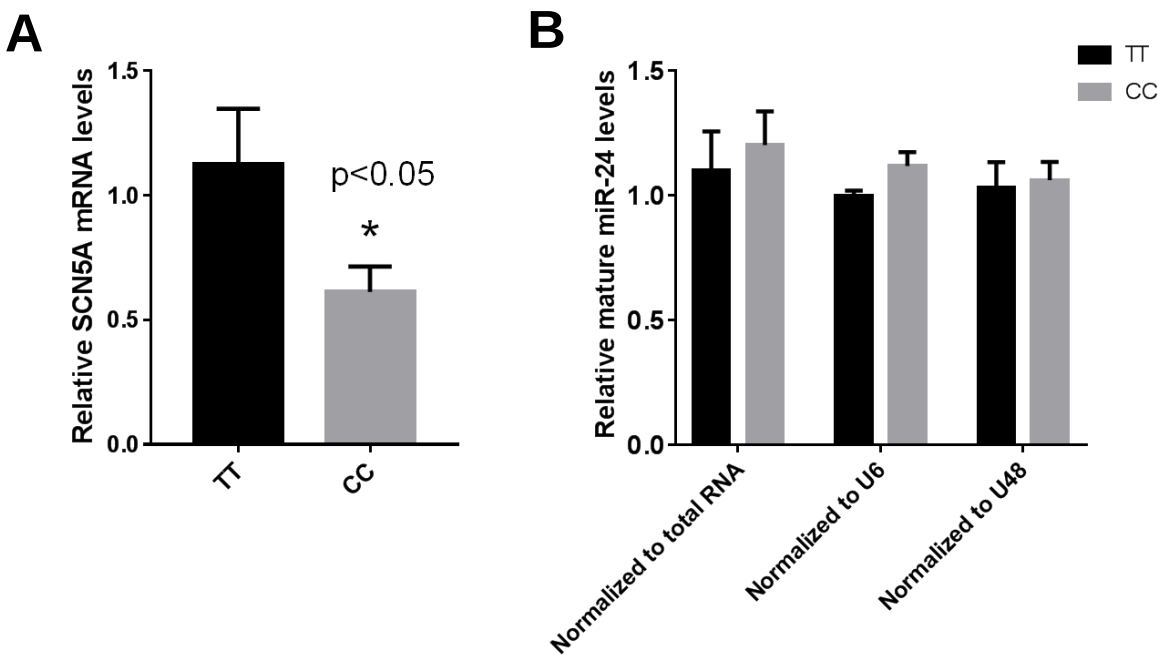


**Supplemental Figure 7. QPCR evaluation of *SCN5A* mRNA and miR-24 levels in non-failing human cardiac tissues used for Figure 4A,B.** Non-failing human cardiac tissues samples (information in Supplemental Table 2) were evaluated by QPCR to compare *SCN5A* (**A**) and mIR-24 (**B**) expression levels in TT (n=7) and CC (n=9) sub-groups based on rs1805126 genotype. *SCN5A* expression was normalized to GAPDH mRNA, and miR-24 was normalized by various means, indicated in the plot. The CC group showed significantly less *SCN5A* expression ($p<0.05$; unpaired two-tailed t-test), and no significant differences were observed for miR-24 levels.

**Supplemental Figure 8**

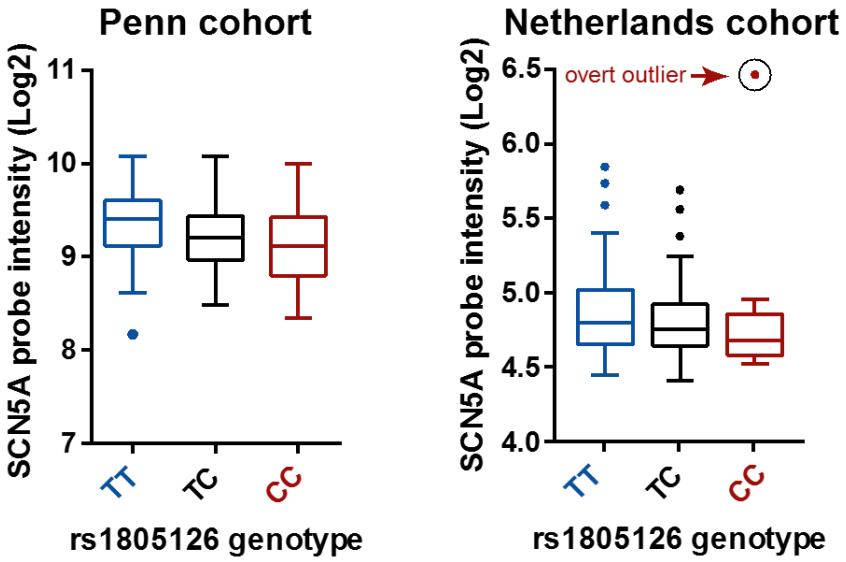


**Supplemental Figure 8. Association of rs1805126 genotype with *SCN5A* mRNA levels in human hearts.** Re-analysis of available genome-wide human cardiac eQTL data from non-failing hearts reveals that CC samples express less *SCN5A* mRNA, compared to TT samples; cohorts from UPenn (left) and Netherlands (right). Normalized microarray probe intensity (Log2) is plotted. These data are an extension of **Figure 4C** to include to the TC group, which shows intermediate expression relative to homozygotes. For Penn, samples numbers are as follows: TT=54, TC=60, CC=22, and for Netherlands: TT=59, TC=55, CC=11. Tukey whiskers are plotted. All data points were included in statistical analyses except for the only overt outlier (circled) flagged by ROUT (definitive stringency, Q=0.1%).

**Supplemental Figure 9**

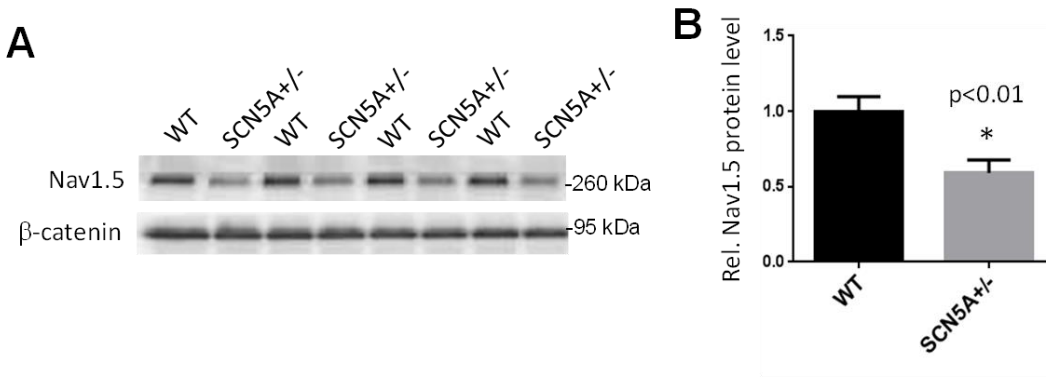


**Supplemental Figure 9. Cardiac Nav1.5 expression levels in *SCN5A* heterozygous knockout mice.** (**A**) Western blot was performed on cardiac tissue lysates harvested from 7-8 month-old *SCN5A* heterozygous knockout (SCN5A+/-) and wild-type littermate mice (n=4 each), and densitometry analysis was used to quantify Nav1.5 expression, normalized to beta-catenin loading control (**B**). P-value was determined by unpaired two-tailed t-test.